

# Development of a monitoring system for air bubbles detection in an internal gears pump

Michele Cotogno<sup>1</sup>, Marco Cocconcelli<sup>1</sup> and Riccardo Rubini<sup>1</sup>

<sup>1</sup>University of Modena and Reggio Emilia, Department of Science and Engineering Methods,  
Via Amendola, 2 – Morselli Building, 42122 Reggio Emilia, Italy  
michele.cotogno@gmail.com, marco.cocconcelli@unimore.it, riccardo.rubini@unimore.it

## Abstract

The presence of air bubbles inside an internal gears pump usually leads to fast pump damage and breaking. When bubbles enter the high pressure chamber they may implode releasing pressure waves in the fluid that ultimately detach material from the gears and other crucial pump parts. This paper recalls and describes the activities performed in order to develop a condition monitoring system able to indicate the presence of air bubbles in an internal gear pump that feeds the hydraulic system of a packaging machine: this pump experienced a breakdown after only 3 minutes of air bubbles flowing in it. Since the machine is supposed to work continuously, an unexpected stop has heavy consequences in terms of loss of production time: therefore the machine producer decided to implement the condition monitoring (CM) of the pump. The producer's goal is to use the warnings/alarms generated by the CM algorithm as a supplemental machine control signal: this may eventually command the stop of the machine to preserve it (and consequently the machine functionality) from fast damaging. The main phases of the development had been: data recording and analysis, diagnostic parameters identification, algorithm development and final algorithm validation in field tests. The data recording campaign included the simultaneous acquisition of 14 quantities of 5 different kinds (vibration, pressure, temperature, electrical torque and angular speed). The data analysis highlighted one of the vibration signals as the most significant to be monitored. Several signal features were analysed in order to evaluate their diagnostic capability (i.e.: the ability to detect the presence of air bubbles in the pump); five features are used by the CM algorithm for the bubbles warning/alarm generation, these being the RMS, the bandpass filtered signal RMS, the Signal Entropy, the Spectral Mean Square Error and the Spectral Cumulative Difference. Currently, the algorithm is being tested and validated on recorded data and a field test campaign is being scheduled.

## 1 Introduction

Hydraulic pumps are one of the most used components in modern industry: because of this, several types of hydraulic pumps have been developed to satisfy the industry requests. This paper is focused on the detection of air flow in a hydraulic internal gears pump which feeds the hydraulic system of a plastic caps forming machine. The cap is formed via the compression of the plastic material in a mould by an hydraulic cylinder: the machine hosts 64 moulds and the relative compression cylinders on a rotating support (or "turntable"), and this arrangement allows a production rate up to 1600 caps/min (at this production rate the turntable rotates at 25 rpm  $\approx$  0.42 Hz). The hydraulic system feeding is provided by two internal gears pumps (separated for high and low pressure oil feeding), which share the inlet port and are coupled on the same driveshaft - the latter being actuated by an electric motor. An internal gears pump (Fig. 1) is basically a gearing with an insulator between the two gears (the input gear with external teeth and the output gear with internal teeth): the rotation of the gears carries the fluid from the inlet to the outlet while increasing the fluid pressure. The insulator (named "filled segment carrier" in Fig. 1) is composed of a static part hosting a mobile part: the mobile part is pressed against the outer gear teeth by three flat springs in order to realize the chambers insulation. Incidentally, the high and low pressure pumps have the same number of teeth, this being 13 for the inner gear and 19 for the outer gear: since they are coupled on the same driveshaft they exhibit the same gearing fundamental frequencies (e.g.: mesh frequency). The machine hydraulic system is quite complex (also due to the hydraulic coupling between the machine static part and the turntable) thus it's possible that some air seepage in the oil occurs. When this happens, the pumps break after few minutes of oil/air mixture flow inside them; during the machine tests this problem manifested and the high pressure pump broke after only 3 minutes of oil and air flowing in it. In Fig. 2 is visible the resulting damage on the pump's internal chambers insulator, which is the most fragile part in this situation.

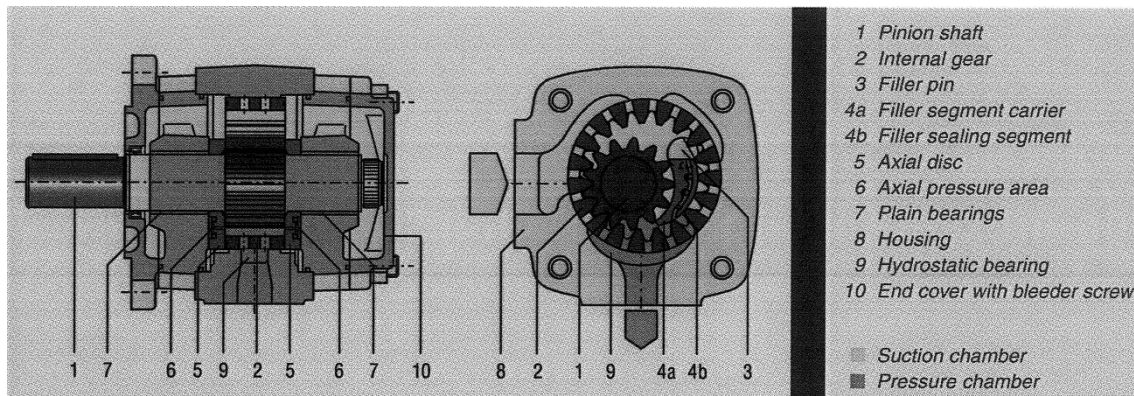


Figure 1: The internal gears pump subject of this paper.

Moreover, the damage originated particles are spread inside the hydraulic system where they can generate further damages: given the complexity of the hydraulic system, along cleaning time is required and consequently there is a large production loss. The machine producer decided that a diagnostic system able to detect the presence of air in the pumps was the best solution to this problem, and some motivations of this choice are the sporadic nature of the fault and its severity on the machine operational time. The producer's goal is indeed to use the warnings/alarms generated by a condition monitoring (CM) algorithm as a supplemental machine control signal: this may eventually command the stop of the machine in case of air flow through the pump to preserve it (and consequently the machine functionality) from fast damaging. This paper is organized as follows: the next section summarizes and describes the experimental campaign and data analysis. Subsequently the chosen diagnostic parameters and their behaviour are presented. Finally, the current version of the pump CM algorithm is illustrated.



Figure 2: The chambers insulator damaged after the second experimental test.

## 2 Experimental tests and setup

A series of three experimental tests was performed with different goals. The recorded physical quantities were triaxial pumps vibrations, pumps inlet pressure (the inlet port is shared by the two pumps), outlets pressures and temperatures and driving motor torque. An extra single axis vibration signal coming from a recirculating pump was also recorded, because this pump was recognized to emit some hissing when air seep in the oil; finally, a tachometric signal – giving one pulse per driveshaft revolution – was recorded besides the aforementioned quantities to perform time synchronous averaging, thus raising the total number of acquired signals to 14 (sampling frequency was 10 kHz per channel). National Instruments hardware and software were used for data acquisition. The pumps behaviour was recorded in all the three main operative modalities of the machine, these being “production” (complete operational state of the machine), “rotation only” (the turntable rotate but the hydraulic cylinders aren't working) and “pump only” (the turntable is stationary; the hydraulic system is fed and pressurized while all the oil flow is routed to the tank). The first test was aimed to the characterization of the pump behaviour in standard conditions (i.e.: no air leakage in the hydraulic system), thus some major operative parameters were changed along the trials (like the production rate, feeding pressure, etc.) inside all the three operative modalities, resulting in a total of 33 trials for this first test. This was done to highlight the differences in the signals behaviour with respect to the widest set of machine operation conditions. The analysis of this set of data permitted to identify two major dynamics, one relative to the speed of the pumps and one to the speed of the turntable. The pumps dynamic

is practically equivalent to typical gear behavior [1, 2, and 3]: mesh frequency and its harmonics dominate the spectra and the other gear fundamental frequencies can be easily observed both in vibration and pressure spectra. The turntable dynamic (Fig. 3) is composed of some notable frequencies that are dependent on the turntable rotation speed  $f_r$ , e.g. the 64<sup>th</sup> harmonic of the latter (i.e.: 26.7 Hz) which represents the oil request by the 64 compression cylinders. This data analysis highlighted a  $af_r$  harmonic that couldn't initially be associated with any known machine event, i.e. the 8<sup>th</sup> $f_r$  harmonic located at 3.3 Hz: a consultation with the machine producer allowed linking this harmonic with the oil request from the 8 high pressure oil feeding channels which route the oil flow from the pumps to the cylinders. All the aforementioned signal features are recognizable in both the vibration and pressure spectra, making these two quantities the most communicative from the diagnostic point of view; indeed, pumps outlets temperature signals don't give any useful information (as expected, because of their slow response) as the driving motor current.

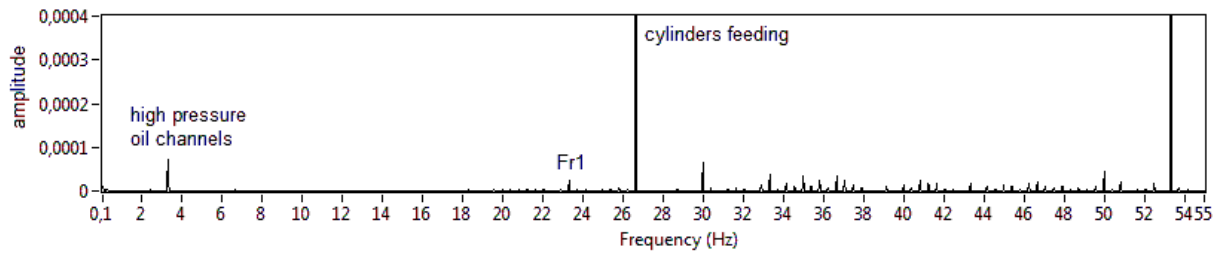


Figure 3: Spectrum of the outlet pressure signal from the high pressure pump. This spectrum is dominated by the turntable hydraulic dynamic. Fr1 identifies the input gear speed.

The second test was aimed to the characterization of the fault and to the identification of signal parameters able to communicate the presence of air in the pumps: this was done by deliberately injecting a known air flow at the pumps suction, which generated air bubbles in the oil. The injected air flow was increased in every trial, starting from 0 l/min to 1.2 l/min with 0.2 l/min increments. Every trial was 30 s long, and was composed of 10 initial seconds of normal operating conditions (i.e.: no air injected) followed by 10 seconds of air injection and final 10 seconds of no air injection: this trial arrangement permits the observation of the transients relative to the entry of air into the pumps and the disposal out of air from them. The recorded quantities were reduced from the first test to only triaxial vibrations of the pumps, pumps pressures, driving motor current, tachometric signal and air injection valve state (i.e.: ON/OFF), all sampled at 10 kHz. Since the fault occurrence is very severe on the pump state only 11 trials were performed, all of them in the “only pumps” machine modality and with the same setting of other major operative parameters (in particular, the rotation speed of the pumps). The data were analysed by means of the Short Time Fourier Transform (STFT, [1]), an analysis technique that gives a time-frequency representation of the signal (i.e.: the Spectrogram) from which is easy to identify the changes of its spectral content along the time. This choice is motivated also by the fact that this powerful tool could be used as a basis for advanced signal features calculation (e.g.: [4, 5, 6]), a further activity performed in this development process. The STFT analysis of this set of data highlights the vibration as the most communicative signature of the presence of air in the pump, confirming as the most efficient and therefore the most used physical parameter to be acquired for the condition monitoring (e.g.: [1,2,3,7,8]). The pump vibration spectrograms (Fig. 4-5) exhibit variations in the amplitudes of the mesh frequency harmonics when air is injected. These variations aren't systematic: if harmonics in one specific trial increase their amplitude when the air flow starts, they may act inversely (i.e.: amplitude decrease) in another trial involved by a different air flow. The parts of the spectrum that lie inside two mesh frequency harmonics exhibit some background noise when the machine operates in normal conditions: the noise level increases systematically when air is injected, and its growth relates to the increase of the injected air flow along the trials (i.e.: greater air flow in the pump induce greater noise in those spectrum areas). The most sensitive vibration directions are the two that lie on the gearing plane (i.e.: the two perpendicular to the pump axis of rotation) of the high pressure pump. In contrast, the pressure and motor current signals appear completely insensitive to the presence of air in the pumps, making them diagnostically useless.

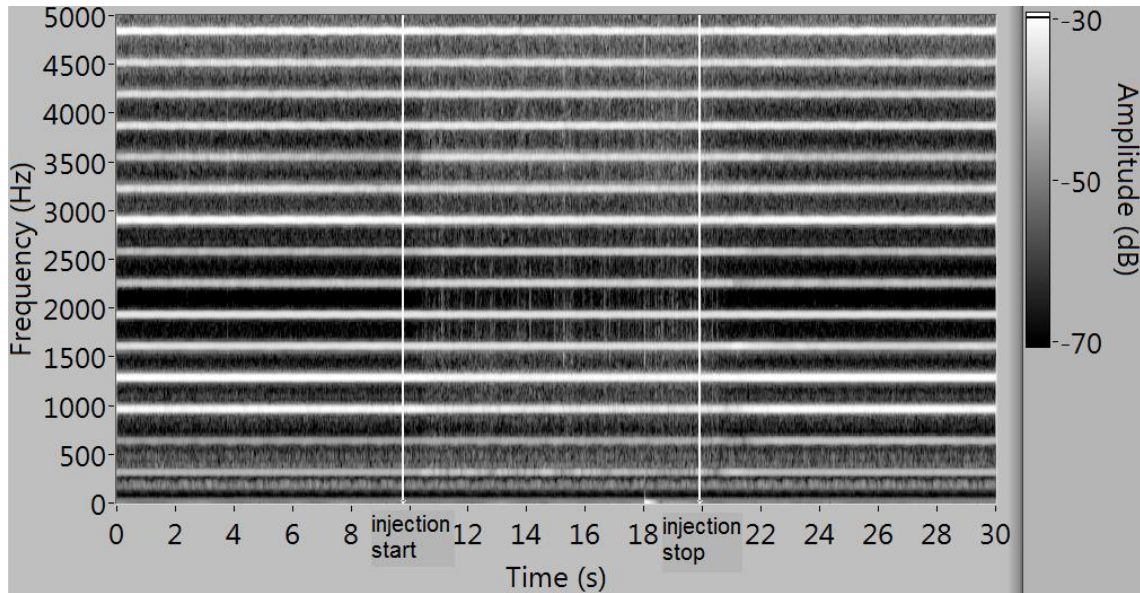


Figure 4: Spectrogram of the vibration of the high pressure pump. The two white vertical lines indicate the air injection start and stop (0.6 l/min in this trial). The dominating frequencies (i.e.: the horizontal lines) correspond to the mesh frequency (324 Hz) and its harmonics.

The last test performed was arranged very similarly to the second test: the differences are the operative modality of the machine (“production” in this third test, “only pumps” in the previous one) and the sampling frequency used to record the signals (raised to 50 kHz). The trials structure and the recorded quantities remained those of the second test. The pumps were subjected to revision before this test, as the previous trials with air injection heavily damaged the pump chambers insulators. The goals of this test were the following: to highlight possible influences of the turntable dynamics on the diagnostic capability of the signals; to build a dataset relative to fault occurrences during complete machine operation to be used in later algorithm developing; to investigate if higher frequencies in the signals spectra could help to communicate the presence of air in the pumps. The data analysis shows that the spectrum behaviour described before replicates itself also in high frequencies, and confirmed the overall signals behaviours. The next step in the development of a pump monitoring system was the identification of some numerical indicators – based on the pump vibration signal – able to communicate the presence of air bubbles: this is treated in the next section.

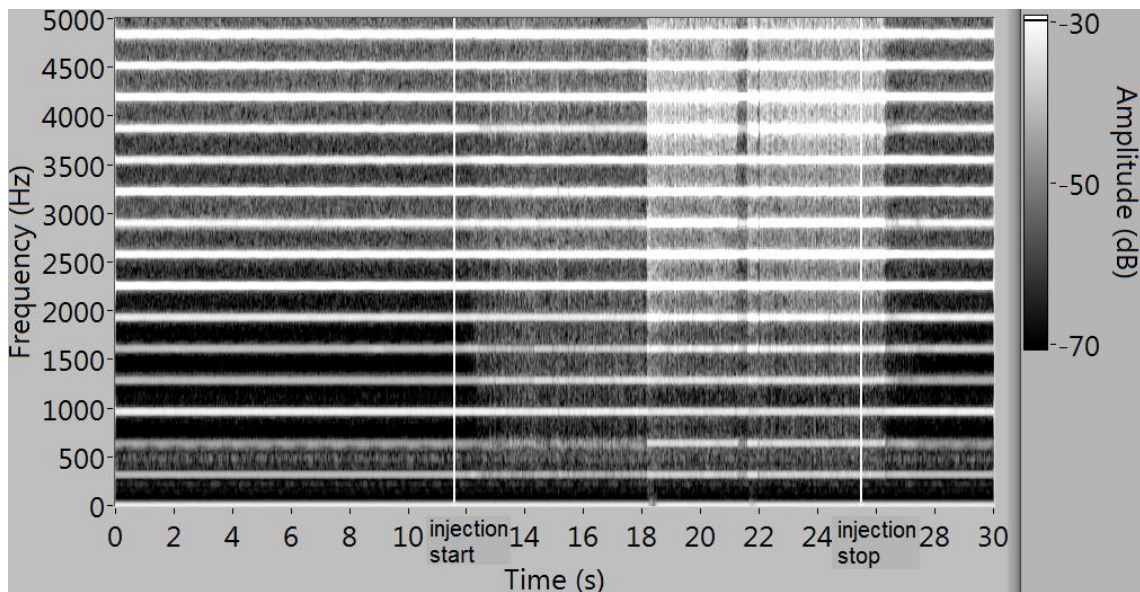


Figure 5: Spectrogram of the vibration of the high pressure pump. The two white vertical lines highlights the air injection start and stop (0.8 l/min in this trial). The dominating frequencies (i.e.: the horizontal lines)

correspond to the mesh frequency (324 Hz) and its harmonics. Notice the increase of the background noise w.r.t. Figure 4 when air is injected.

### 3 Diagnostic parameters

The numerical indicators that can highlight the presence of air bubbles in the pumps must be calculated on-line by a diagnostic algorithm, which was decided to operate on a segment of vibration signal. In order to reduce the overall diagnostic system cost, it has been chosen to monitor only the vertical axis of vibration lying on the gearing plane: the experimental data analysis indeed shows that this is the most sensible axis from a diagnostic point of view. The temporal length of vibration segment must be chosen appropriately in relation with the rapidity of the fault developing: in this case the air flow presence leads to machine failure in 3 minutes (worst case experienced), so the segment duration was chosen to be less than 1 second, giving the algorithm the possibility of checking the pump status at least 180 times in the worst case. Given this requisite, the parameters have been investigated both in their diagnostic ability and in their dependence from the duration and sampling frequency of the vibration signal segment. This research resulted in the identification of the following 5 vibration signal parameters: RMS (Eq. 1), Shannon Entropy (E, Eq. 2), bandpass filtered signal RMS (FRMS, Eq. 3), Spectral Cumulative Difference (SCD, Eq. 3) and the Spectral Mean Square Error (SMSE, Eq. 4). In these equations,  $x(t)$  is the actual vibration signal segment and  $n$  is its samples number,  $x_f(t)$  is the bandpass filtered  $x(t)$ ,  $X(f)$  is the autospectrum of  $x(t)$  and  $N = n/2$  is its frequency bins number, and  $\overline{X(f)}$  is a reference autospectrum relative to machine in standard condition. In Equation 2, if  $x(t) = 0$  the convention  $0 \cdot \ln 0 = 0$  is used; the filtering band for FRMS calculation has been chosen to be 4 ÷ 8 kHz: in this frequency band the aforementioned increase of the background noise showed to be stronger during the trials.

$$RMS = \sqrt{\frac{1}{n} \sum_n x^2(t)} \quad (1)$$

$$E = \sum_n [x^2(t) \ln x^2(t)] \quad (2)$$

$$FRMS = \sqrt{\frac{1}{n} \sum_n x_f^2(t)} \quad (3)$$

$$SCD = \sum_N |\overline{X(f)} - X(f)| \quad (4)$$

$$SMSE = \frac{1}{N} \sum_{N-1} [\overline{X(f)} - X(f)]^2 \quad (5)$$

In Figure 6 the behaviour of the RMS is shown; this behaviour is qualitatively the same of the other chosen parameters, which is a “standard condition” (healthy) value which changes regularly when there is air flow in the pump. The parameters exhibit different values for the same standard condition but in different trials: this is probably due to the fact that before the tests the machine was initially off, so the trials were performed during its warm-up phase. For example (Fig. 6), in the first trial of the third test the RMS with no air flow in the pumps is about 1.8, while in the last trial it is about 1.5 (same test, same “no air flow” condition). Since the machine could reach different regimen temperatures (depending on the environmental conditions and other factors) a simple parameter threshold check doesn’t appear as a robust diagnosis method; moreover, recalling the previous RMS example, the “healthy” RMS value of 1.5 in the last trial corresponds to a “faulty” RMS value in the first trial – and this occurs to the other parameters too.

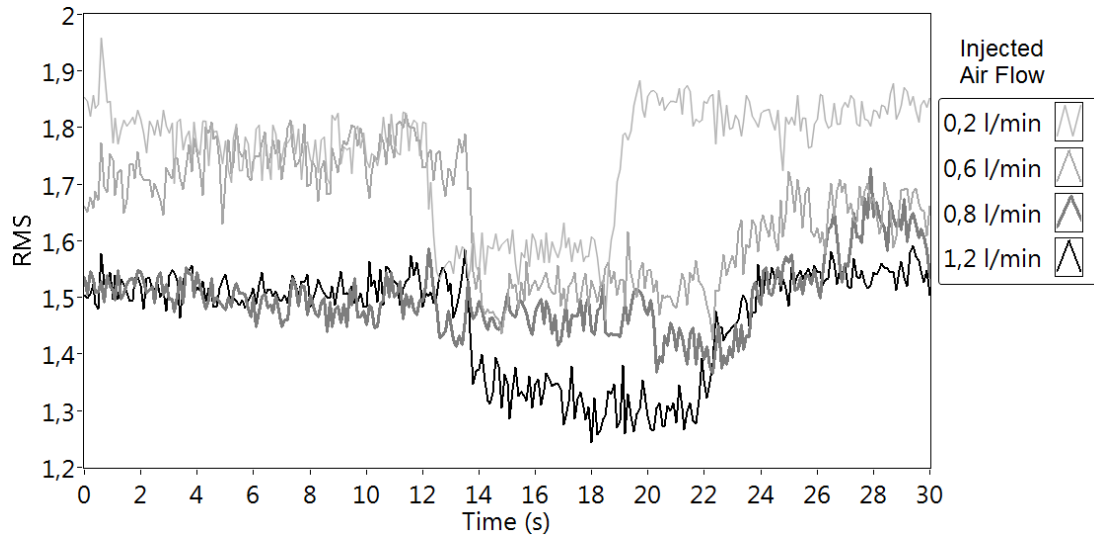


Figure 6: Pump vibration RMS evolution. Each graph relates to a different trial from the third test (the graph legend lists the trials in chronological order of execution). Since the air injection valve was commanded manually, the moments of injection start and stop are slightly different in each trial: nevertheless, the presence of air is easily recognizable as a distinct RMS variation in each graph central area. Notice that the “healthy” values (i.e.: those at the beginning and at the end of the graph) drop from a trial to the next one, probably because of the machine warm-up.

In order to overcome this issue it was decided to base the diagnosis on the comparison of the percentage variations of the parameters value (with respect to a healthy reference value) with an appropriate threshold. The healthy reference value is obtained with an appropriate calibration operation at every machine start (this is discussed in detail in the next section). This arrangement makes the percentage variations of the parameters a much more robust indicator of the pump flow status than the sheer parameters values. The influence of the vibration segment duration ( $T$ ) and sampling frequency ( $f_s$ ) on the parameters behaviour was studied in all the 4 combination  $T \cdot f_s$  resulting from taking  $T = 0.1$  and  $0.5$  s and  $f_s = 10$  and  $50$  kHz: no particular influence was found, so the final values for the vibration segment were chosen as  $T = 0.1$  s and  $f_s = 10$  kHz. With this choice the algorithm will be able to check the pump status at least 1800 times in the worst case; this choice of  $T$  and  $f_s$  gives also  $n = 1000$  and  $N = 500$  in Equations 1-5, and limits the filtering band for the FRMS calculation to  $4 \div 5$  kHz without diagnostic performance loss. The next section illustrates how these parameters are used by the algorithm to perform the diagnosis.

#### 4 Diagnostic Algorithm

The diagnostic algorithm flowchart is reported in Figure 7. The input is the vibration signal segment and the output is a Boolean variable which is “true” when there is air flow in the pumps. This is the basic algorithm and will probably be passible of some modifications in its (still on-going) developing. The algorithm steps are the following: first of all the diagnostic parameters are evaluated; if calibration is required or been performed, the parameters values contribute to the references creation, otherwise the diagnosis is performed. The latter is done by comparing the parameters percentage variations (w.r.t. their reference values) with their relative thresholds: this comparison generates a “pre-alarm” flag for every parameter which is “true” when the variation is greater than the threshold. The 5 pre-alarm flags are converted from “true/false” to “1/0” values and then weighted summed: this weighted sum ( $S$  in Fig. 7) is finally compared to a “global” threshold for the diagnosis generation (i.e.: the output Boolean variable), which will be “true” (meaning: “air flow in pumps”) when the weighted sum is greater than the global threshold. The last algorithm step is the parameters references update.

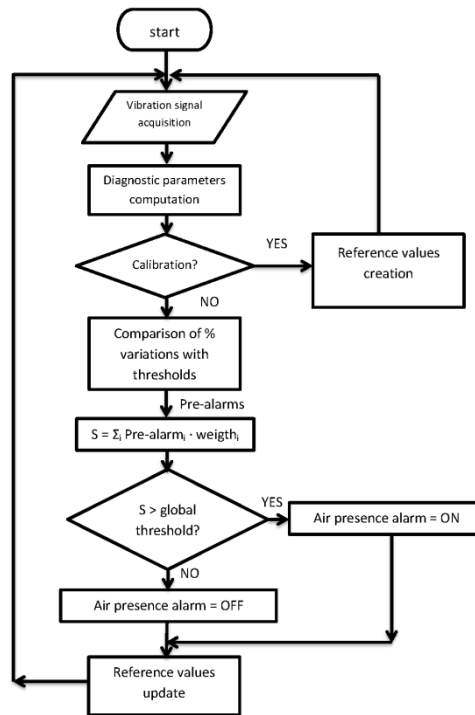


Figure 7: The Condition Monitoring Algorithm flowchart.

In the present algorithm version, the parameters references are obtained as the average of the first  $n_r$  values of each parameter; for the spectrum dependant parameters (SCD and SMSE) the reference is the spectrum  $\overline{X(f)}$  which is obtained as the average of the first  $n_r$  calculated spectra. Similarly, the references update is obtained by a mobile average of the last  $n_r$  parameter values ( $n_r$  has been set to 70 in the actual algorithm version). The calibration phase is set to be automatically performed at the first algorithm execution (i.e.: at every algorithm/machine start), but it can be also performed on demand by an operator command: in both cases, to obtain a correct calibration it must be assured that the machine is working correctly, i.e. without air flow in the pumps. This references management solution should consent the algorithm to adapt and function correctly also when the machine regimen condition is different to the one experienced during the tests, but it has the main drawback of being modestly sensible to slow developing faults: indeed, if  $n_r$  is set to be large, a slow but constant percentage variation of the parameter could be absorbed in the mobile averaging without shifting to “true” its relative pre-alarm. This is crucial because in the actual algorithm form, a parameter reference update is done only if that parameter’s pre-alarm is false: for example, if the RMS percentage variation is greater than the RMS threshold, the actual RMS value will not be included in the mobile averaging calculation and consequently the RMS reference value will not be updated. This references updating politic is very simple and has its own limitations, but it can be easily modified (by changing few logic conditions in the program) in future developing if needed. The parameters thresholds, the parameters weights for the weighted sum, and the global threshold have been obtained manually by the developers by means of a kind of “algorithm tuning”, based on the dataset obtained in the third test. Figure 8-10 shows some comparisons of the algorithm diagnoses and the air injection valve command: it can be seen how the pump status is correctly estimated in every condition.

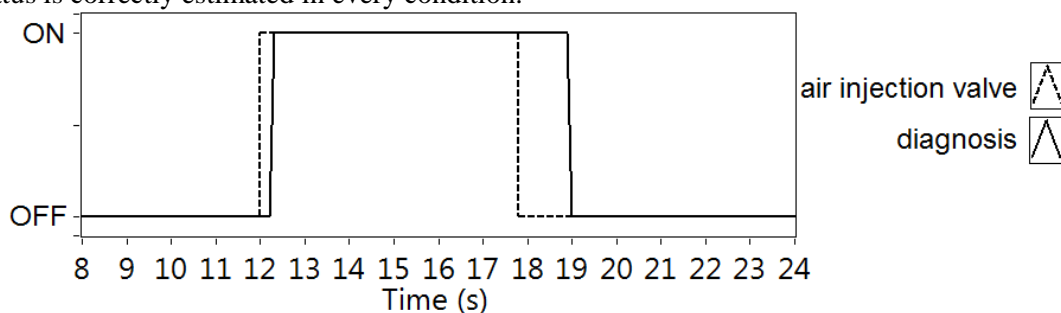


Figure 8: Comparison of the algorithm diagnoses and the air injection valve command. In this trial the injected air flow was 0.2 l/min, i.e. the smallest tested. The algorithm diagnosis is correct.

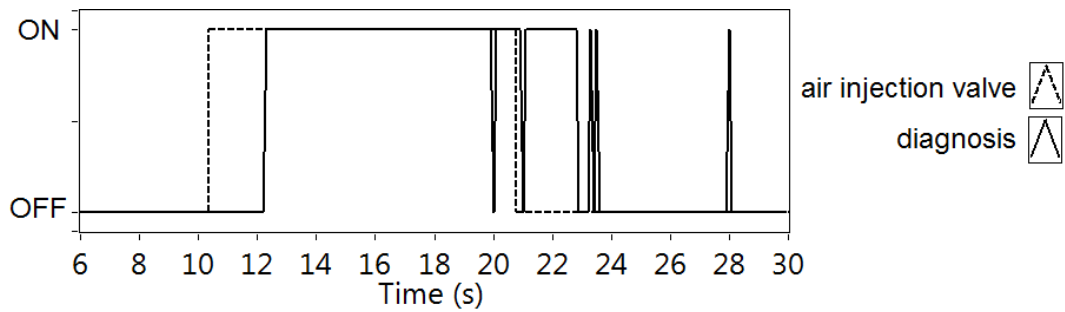


Figure 9: Comparison of the algorithm diagnoses and the air injection valve command. In this trial the injected air flow was 0.8 l/min. The diagnosis isn't perfect (e.g.: alarm is erroneously OFF at  $t = 20\text{ s}$ ) but acceptable: indeed, this is the most difficult case to diagnose because the diagnostic parameters exhibit the most irregular behaviour with this particular air flow.

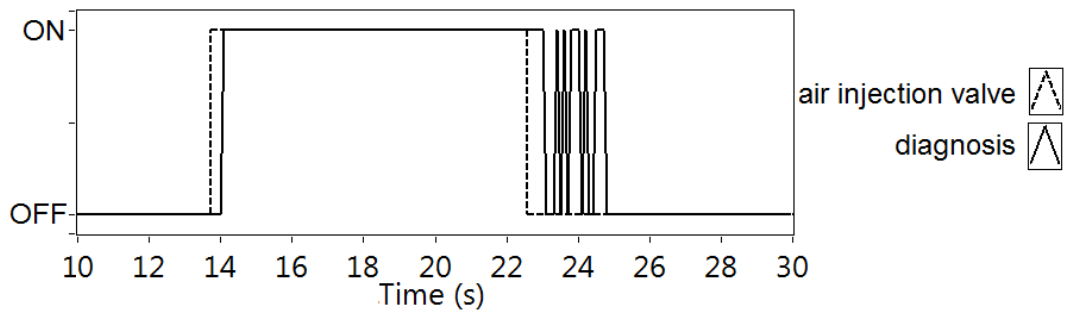


Figure 10: Comparison of the algorithm diagnoses and the air injection valve command. In this trial the injected air flow was 1.0 l/min. The algorithm diagnosis is correct: the alarm state oscillations visible around  $t = 24\text{ s}$  are relative to the last air bubbles exiting the pump.

The visible lag between the opening command of the valve and the algorithm output transition from “false” to “true” corresponds to the time needed for the injected air flow to travel from the injection point to the pump, thus this lag is negligible in practice; similarly, the oscillations visible on the output after the valve closing command are relative to the air flow disposal out of the pumps (i.e.: residual bubbles passing through the pumps), which is not immediate. These two lags are also visible in the spectrograms reported in Fig. 4 and Fig. 5. When the injected air flow is equal to 0.8 l/min some oscillations of the output occur when the valve is open, thus giving some erroneous diagnoses: indeed this particular amount air flow causes an irregular behaviour of the 5 diagnostic parameters (an example is visible in Fig. 6), resembling a kind of hydro-mechanical resonance condition of the pump.

## 5 Conclusions and future work

A diagnostic solution for air flow detection in an internal gears pump has been developed. The methodology used in the development process has been exposed. In its current version, the Condition Monitoring algorithm is able to correctly identify the presence of air bubbles in the available datasets. Currently the test bench does not allow to evaluate the efficiency of the algorithm in case of slow developing faults, frequently arising inside the machine hydraulic systems, therefore further investigations are required. In order to verify the CM algorithm behaviour in this case, a further experimental test is being set up by the machine producer: the air injection will be gradual and slightly increasing and will not be stopped until the oil in the tank will be completely mixed with air, i.e. the tank will be full of foam. Authors propose two possible extensions of the algorithm to monitor slow air seepages: the re-tuning of the algorithm to obtain a new set of thresholds and parameters weights able to identify this kind of infiltration by preserving, if possible, the identification of “fast” faults; alternatively the solution may be to add an additional Boolean output which will be specific for “slow” faults. The generation of this output might be identical to the one presented in the previous section, but it will have an own set of parameters thresholds and weights. By doing this, two alarms will be available for the machine operator (or the machine control system) which will dedicated to highlight the presence of a “fast” (i.e.: “step-like”) or “slow” (“ramp-like”) air seepage in the hydraulic system.



## Acknowledgements

The authors wish to thank the Inter Departmental Research Centre INTERMECH MoRE of the University of Modena and Reggio Emilia for the financial support.

## References

- [1] R. B. Randall, *Vibration-based Condition Monitoring: Industrial, Automotive and Aerospace Applications*, John Wiley and Sons, West Sussex, (2011).
- [2] A. G. Piersol, T. L. Paez, *Harris' Shock and Vibration Handbook – 6<sup>th</sup> edition*, McGraw Hill, New York, (2010).
- [3] J. I. Taylor, *The Vibration Analysis Handbook – 2<sup>nd</sup> edition*, Vibration Consultants, United States, (2003).
- [4] J. Antoni, *The spectral kurtosis: a useful tool for characterising non-stationary signals*, Mechanical Systems and Signal Processing, 2006, Vol.20, No. 2, Elsevier (2006), pp. 282-307.
- [5] M. Cocconcelli, R. Zimroz, R. Rubini, W. Bartelmus, *Kurtosis over Energy distribution approach for STFT enhancement in ball bearing diagnostics*, Proceedings of the 2<sup>nd</sup> International Conference on Condition Monitoring of Machinery in Non-Stationary Operations, Hammamet, Tunisia, 2012 March 26-28, (2012).
- [6] M. Cocconcelli, R. Zimroz, R. Rubini, W. Bartelmus, *STFT based approach for ball bearing fault detection in a varying speed motor*, Proceedings of the 2<sup>nd</sup> International Conference on Condition Monitoring of Machinery in Non-Stationary Operations, Hammamet, Tunisia, 2012 March 26-28, (2012).
- [7] W. Bartelmus, R. Zimroz, "Vibration condition monitoring of planetary gearbox undervarying external load", Mechanical Systems and Signal Processing, Vol. 23, No. 1, Elsevier (2009), pp. 246-257.
- [8] T. Barszcz, "Validation of vibration measurements for heavy duty machinery diagnostics," in *Proceedings of 1<sup>st</sup> Conference on Condition Monitoring of Machines in Non-stationary Operations*, Wroclaw, Poland, 2011 March 7, (2011).